Available online at http://www.ijprt.org.tw/

Chinese Society of Pavement Engineering

International Journal of Pavement Research and Technology 11 (2018) 698-708

http://www.ijprt.org.tw/

Gray relational entropy analysis of high temperature performance of bio-asphalt binder and its mixture

Junfeng Gao [a], Hainian Wang [a,*], Zhanping You [b], Xu Yang [c]

[a] School of Highway, Chang'an University, South Erhuan Middle Section, Xi'an, Shaanxi 710064, China
[b] Department of Civil and Environmental Engineering, Michigan Technological University, 1400 Townsend Drive, Houghton, MI 49931, USA
[c] School of Engineering, Monash University, Sunway Campus, Jalan Lagoon Selatan, 47500 Bandar Sunway, Malaysia

Received 7 September 2017; received in revised form 9 February 2018; accepted 10 February 2018

Abstract

Most of the existing researches only focus on some performances of the bio-asphalt binders instead of the asphalt mixtures, and the relationship between the performance of bio-asphalt binder and the performance of the mixture has been rarely reported. To analyze the gray relational entropy of high temperature performance of bio-asphalt binder and mixture, the bio-asphalt modified by 1% SBS with the concentrations of 0% (50#), 5%, 10%, 15%, and 20% by the weight of bio-asphalt binder, respectively, was used in this study. The performance indexes of bio-asphalt binder were tested through the conventional performance test and Superpave test of asphalt. The correlation between the performance indexes of the asphalt binder and the dynamic stability of the mixture was studied through the gray relational entropy method. The results showed that the high temperature performance of bio-asphalt had a certain degree of reduction before RTFO with the incorporation of bio-oil. The binder test parameters showed different changes in the law with the changes of bio-oil content. The dynamic stability of bio-asphalt mixtures decreased with an increase in bio-oil content. The RTFO aging had a great influence on the entropy correlation between the performance indexes of the bio-asphalt binders and the dynamic stability of the mixture. The non-recoverable creep compliance of bio-asphalt with low content (1%) of SBS modifier was weakly correlated with the dynamic stability of the mixture. The dynamic viscosity of bio-asphalt and the dynamic stability of the mixture exhibited the highest gray entropy correlation, which could be used as the key index of high-temperature performance evaluation of bio-asphalt.
© 2018 Chinese Society of Pavement Engineering. This is an open access article under the CC BY-NC-ND license (http://creativecommons.org/licenses/by-nc-nd/4.0/).

Keywords: Road engineering; High temperature performance; Gray relational entropy; Bio-asphalt

1. Introduction

1.1. Background

With the development of asphalt pavement technology, and the increase in highway pavement construction and maintenance, the demand of asphalt materials has been overall rising in the past decades. At the same time, the oil resources used to produce petroleum asphalt are also declining. Therefore, seeking alternative asphalt materials has become the focus of the current road engineering [1]. In a variety of renewable energies, biomass energy has good advantages such as wide distribution and large reserves, etc. [2,3]. And biomass could be used to extract bio-oil for further processing. The bio-oil could be mixed with petroleum asphalt or added some additives under different conditions, thus the bio-asphalt could be made, which has become a new material in the field of pavement engineering. The environmental concerns and the

* Corresponding author.
E-mail addresses: gaojunfeng@chd.edu.cn (J. Gao), wanghn@chd.edu.cn (H. Wang), zyou@mtu.edu (Z. You), xu.yang@monash.edu (X. Yang).
Peer review under responsibility of Chinese Society of Pavement Engineering.

https://doi.org/10.1016/j.ijprt.2018.02.001
1996-6814/© 2018 Chinese Society of Pavement Engineering.
This is an open access article under the CC BY-NC-ND license (http://creativecommons.org/licenses/by-nc-nd/4.0/).

compatibility of bio-oil with petroleum asphalt have also been explored in previous studies [4].

In recent years, there has been much research on materials about bio-oil. Fini et al. employed the short-term aging properties of bio-asphalt prepared from pig manure as raw material. The results showed that the viscosity of bio-binders decrease more compared with the base binders after rolling thin film (RTFO) [5–7]. Onochie et al. studied the high-temperature viscosity and rheological behavior of composite modified bio-asphalt prepared with nano-clay and nano-silica. The results indicated that the addition of nano-clay to the bio-modified asphalt improved its high temperature performance [8]. Yang et al. evaluated the mechanical performance of asphalt binders and mixtures modified by bio-oils generated from waste woods [9,10]. Raouf et al. tested the high temperature of bio-asphalt binder properties prepared from oak flour, switch grass, and corn stover. It was found that the viscosity of bio-binder was affected by the bio-oil type during the first test hour and the viscosity results were affected by the bio-oil type, the modifier type and the temperature [11,12]. Wang et al. studied the complex shear modulus, phase angle, rutting factor and viscosity of bio-asphalt. The research showed that the high temperature performances of bio-binder decreased with the increase in bio-oil content and testing temperature when the testing temperature was below than 135 °C [13,14]. He et al. conducted tests for penetration, softening point and ductility among other conventional properties of modified bio-asphalt. The test results indicated that the high temperature performance of two kinds of bio-asphalt is good based on the analysis of the temperature stability of modified bio-asphalt [15]. Rodrigo et al. studied the relationship between nonlinearity of asphalt binders using a Dynamic Shear Rheometer and asphalt mixtures permanent deformation using cylindrical samples. The results showed that there is a strong correlation between the mixture nonlinearity and the binder nonlinearity [16]. Sungun et al. analyzed the relationship of three binder properties with three rutting test data using correlation (R^2). It was found that the binder properties could be reliably used for the estimation of the rut potential of asphalt mixtures [17]. Although more extensive researches has been done on bio-asphalt in recent years and some researches on the relationship between asphalt binder and mixture were also done, most of the existing literatures focus on the bio-asphalt binders instead of the asphalt mixtures, especially the relationship between the performance of bio-asphalt binder and the performance of the mixture has been rarely reported.

Based on the current research status, this paper aims to test the performance indexes of bio-asphalt binder and study the correlation between the performance indexes of the asphalt and the dynamic stability of the mixture. The performance indexes of bio-asphalt binder were evaluated through the conventional performance test and Superpave test of asphalt. The correlation was determined by the gray relational entropy method. This study will provide a more systematic perspective for the further study of the high temperature performance evaluation of bio-asphalt.

1.2. Objective

The main objective of this study is to evaluate the high temperature performance of bio-asphalt binder and to analyze the gray relational entropy of high temperature performance of bio-asphalt binder and mixture. The bio-asphalt binders were produced in the laboratory incorporating 1% content of SBS and four concentrations (5%, 10%, 15%, and 20% by the weight of bio-asphalt binder) into the virgin asphalt. The performance indexes of bio-asphalt binder were tested through the conventional performance test and Superpave test of asphalt. The dynamic stability of the mixture was tested through rutting test. The correlation between the performance indexes of the asphalt binder and the dynamic stability of the mixture was studied through the gray relational entropy method. Fig. 1 shows the flow chart of the experimental and analyzing procedures followed in this study.

2. Materials and test program

2.1. Materials and mixtures design

2.1.1. Bio-asphalt

A 50 penetration grade virgin asphalt binder (denoted as 50#) taken from a construction site in Maoming, China was used in this study. The styrene–butadienestyrene (SBS) modifier type was 1301-1, and its performance indicators are shown in Table 1. The bio-oil (Fig. 2) was extracted from wood chips, and it was produced by Toroyal New Energy Company located in Shandong province, China, its viscosity is 0.895 Pa·s at 135 °C. The bio-asphalt was prepared from the above raw materials, such as virgin asphalt, SBS and bio-oil. The content of SBS was 1% (by mass fraction) of virgin asphalt, it was mixed with virgin asphalt, and SBS modified asphalt was made. Then 5%, 10%, 15%, and 20% of the bio-oil was mixed with prepared SBS modified asphalt, respectively, which were named as S105, S110, S115 and S120, respectively. The asphalt containing only 1% SBS without bio-oil was named S100.

2.1.2. Aggregate and filler

The coarse and fine aggregates used in this study were limestone in Luquan, Hebei Province, China, and the filler was grinded from limestone. The technical indices of the aggregates are shown in Tables 2 and 3.

2.1.3. Mixtures design

The gradation of asphalt mixture is shown in Table 4. The optimum asphalt content was determined to be 4.3% through the Marshall test based on the test method [18]. Further, the performance tests of the asphalt mixture were conducted.

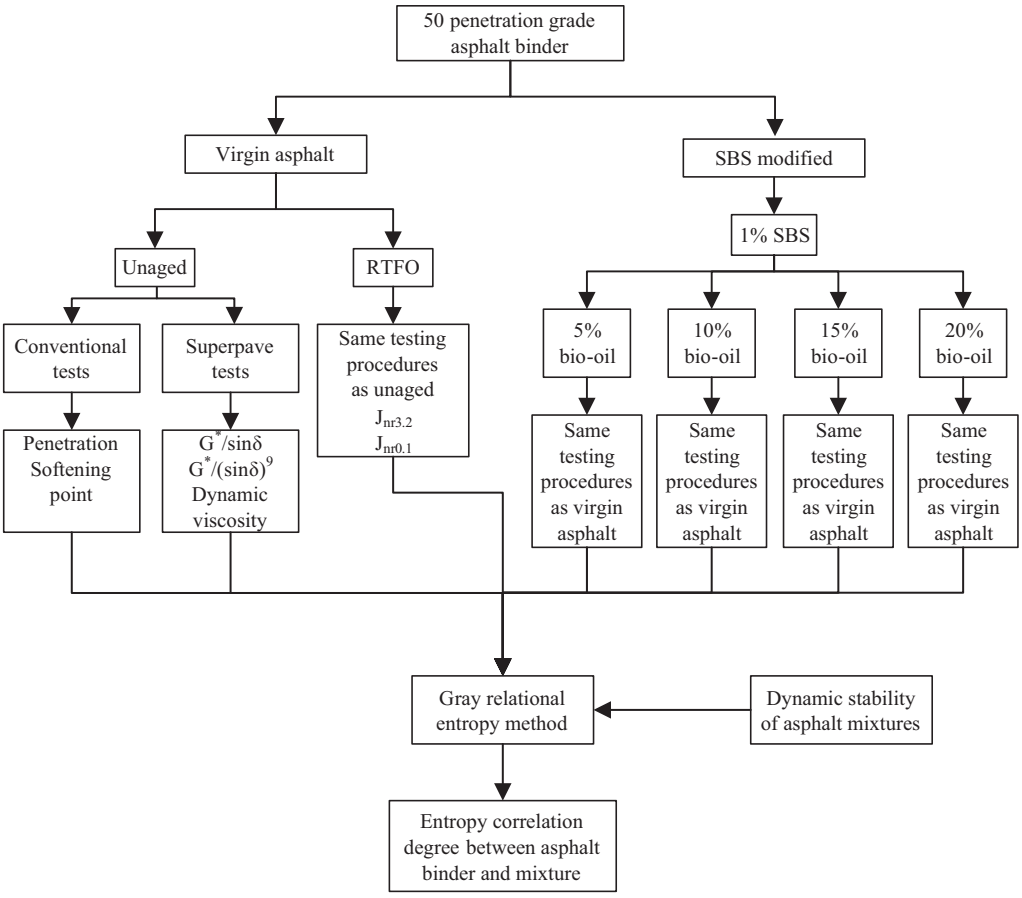

Fig. 1. Flow chart of the experimental and analyzing procedures.

Table 1
Performance indicators of SBS.

Density (25 °C) (g/cm^3)	Tensile strength (MPa)	Ultimate Elongation (%)	S/B (mass ratio)
0.92	18	700	30/70

Fig. 2. Bio-oil.

2.2. Test program

2.2.1. Binder test

The indexes that could better characterize the high temperature performance of asphalt binder were selected, and the influence of the bio-asphalt's aging on its performance was also considered, the dynamic viscosity at 135 °C, penetration and softening point before and after rolling thin film oven (RTFO) were measured according to the standard test methods [19]. At the same time, the Superpave performance indicators including rutting factor $G^*/\sin\delta$ and the modified rutting factor $G^*/(\sin\delta)^9$ proposed by Aroon Shenoy [20] before and after RTFO were measured and calculated. Because the change of $(\sin\delta)^9$ to phase angle (δ) is more sensitive than the change of $\sin\delta$, besides the lower the temperature, the greater the difference in sensitivity, $G^*/(\sin\delta)^9$ is better able to characterize the changes of phase angle (δ) and better to reflect the changes of high temperature performance of asphalt binder.

Table 2
Technical indices of coarse aggregates.

Technical indices	Requirements	Test results of coarse aggregate		
		10–20/mm	5–10/mm	3–5/mm
Apparent relative density	≥2.60	2.687	2.697	2.694
Water absorption/%	≤2.0	1.0	1.0	0.5
<0.075 mm particles content/%	<1.0	0.2	0.2	0.2
Elongated content	≤18	6	6.2	3.4

Table 3
Technical indices of fine aggregate.

Technical indices	Test results	Requirements
Apparent relative density	2.732	≥2.5
Sand equivalent/%	80	≥60
<0.075 mm content/%	9.5	≤10

In addition, the irreversible creep compliance $J_{nr0.1}$ and $J_{nr3.2}$ of virgin asphalt and bio-asphalt at 0.1 kPa and 3.2 kPa stress were tested and calculated through multiple stress creep recovery tests (MSCR) based on AASHTO TP 70-10 [21]. The MSCR test device is shown in Fig. 3. The multiple stress creep recovery test process is as follows: Two levels of creep stress such as 0.1 kPa and 3.2 kPa were used for continuous testing, each stress level loads for 10 cycles, each cycle lasts for 10 s, which was divided into 1 s creep stage and 9 s unloading recovery stage, the duration of the test is 200 s. The device automatically collects the strain data for each creep recovery cycle. The ratio of residual strain to creep stress is defined as unrecoverable creep compliance through the time–strain change graph obtained by the experiment. The unrecoverable creep compliance was calculated for each different cycle according to Eq. (a). Test temperature was selected as 64 °C for it is closer to the actual high temperature of road surface. The MSCR test has been applied to evaluate the high temperature performance of asphalt modified by bio-oil generated from waste wood and to compare with the dynamic shear rheometer (DSR) test [22].

$$J_{nr} = \frac{\varepsilon_{nr}}{\tau} \quad \text{(a)}$$

wherein ε_{nr} is residual strain, and τ is creep stress.

2.2.2. Mixture test

The rutting test is a good method to evaluate the high temperature performance of asphalt mixture. It has been shown that the dynamic stability of rutting can reflect the rutting resistance of asphalt mixture. Therefore, the rutting test for the control asphalt and bio-asphalt mixtures was conducted at 60° C according to standard test [19].

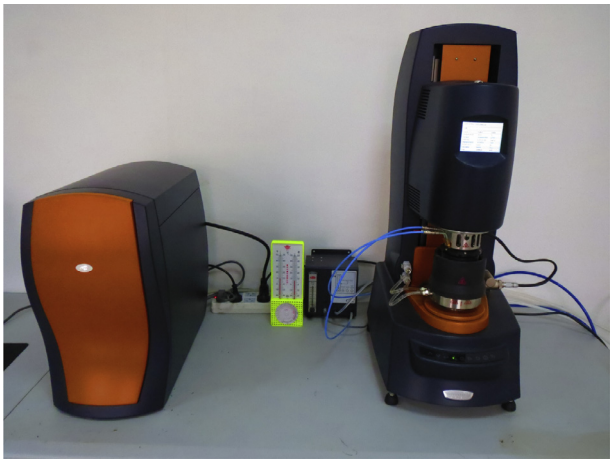

Fig. 3. MSCR test device.

3. Gray relational entropy analysis method

The gray relational analysis is the factor analysis of the system, which is based on the difference or similarity of the development trend of the system factors to measure the correlation between the factors and the system behaviors [23]. The gray relational entropy analysis method was improved on the basis of the gray correlation analysis method [24]. The gray correlation analysis method is to take the simple arithmetic average of the gray correlation coefficients at each time point as the gray relational degree, which will cause the loss of information and the tendency that the local point measurement value controls the whole gray relational order. The method of gray relational entropy can effectively control the influence of the local point correlation coefficient on the entire sequence correlation degree [25]. So by using the method of gray relational entropy, it is possible to avoid the loss caused by the gray relational degree when it is determined. Therefore, it can be more effective to distinguish the main and secondary factors which have the impact on the entire system. Based on its characteristics, this method has been applied in the researches of bio-asphalt binder and bio-asphalt mixtures [26,27].

Table 4
Gradation of asphalt mixture in this study.

Sieve size/mm	19	16	13.2	9.5	4.75	2.36	1.18	0.6	0.3	0.15	0.075
Passing rate/%	100	95	88	75	47	32	23	17	12	8.5	6

3.1. Gray correlation degree

The steps used to calculate the gray correlation degree are listed as follows:

Step 1: Selection of reference sequence and comparison sequence

Evaluation data were collected and matrix ($n \times m$) was established. X is defined as the gray correlation factor set. X_0 is defined as the reference sequence, Xi is defined as the comparison sequence.

$$X_0 = \{X_0(k)|k = 1,2,\ldots,n\} = \{X_0(1),X_0(2),\ldots,X_0(n)\} \tag{1}$$

$$X_i = \{X_i(k)|k = 1,2,\ldots,n\} = \{X_i(1),X_i(2),\ldots,X_i(n)\}(i = 1,2,\ldots,m) \tag{2}$$

Step 2: Normalization of reference sequence and comparison sequence

It is difficult to compare different factors directly, because the dimension of different factors in system is not always consistent and the order of magnitude of different values has a great difference. Therefore, normalization is necessary for eliminating the dimension influence [28,29]. The equalization method was adopted for dimensionless treatment and normalization. X_0 and X_i were processed, and the sequence of numbers is as follows:

$$X_i' = \{X_i(k)|\overline{X}_i|k = 1,2,\ldots,n\}(i = 0,1,2,\ldots,m) \tag{3}$$

Step 3: Calculation of the correlation coefficient

The correlation coefficient between X_i and X_0 is:

$$r_i(k) = \frac{\min\limits_i \min\limits_k |X_0(k) - X_i(k)| + \xi \max\limits_i \max\limits_k |X_0(k) - X_i(k)|}{|X_0(k) - X_i(k)| + \xi \max\limits_i \max\limits_k |X_0(k) - X_i(k)|} \tag{4}$$

wherein, $|X_0(k) - X_i(k)\}|$ is the absolute difference of $X_0(k)$ with $X_i(k)\}$; $\min\limits_i \min\limits_k |X_0(k) - X_i(k)|$ is the minimum of the minimum absolute difference; $\max\limits_i \max\limits_k |X_0(k) - X_i(k)|$ is the maximum of the maximum difference; ξ is a distinguishing coefficient which is changed from 0 to 1, and the value of ξ is usually assumed as 0.5. The correlation coefficient is a reflection of the distance between two points.

3.2. Gray correlation entropy

To calculate the gray correlation entropy, there are two steps listed as follows:

Step 1: Calculation of density value of distribution

X is the discrete sequence, $x_0 \in x$ is the reference sequence, $x_1 \in x(i = 1,2,\ldots,m)$ is the comparison sequence,

$$R_i = r_i(k) = \{r[x_0(k),x_i(k)]k = 1,2,\ldots,n; i = 1,2,\ldots,m\} \tag{5}$$

$$P_h \triangleq \frac{r[x_0(k),x_i(k)]}{\sum\limits_{k=1}^{n} r[x_0(k),x_i(k)]}, P_h \in P_i(h = 1,2,\ldots,n) \tag{6}$$

wherein P_h is density value of distribution.

Step 2: Introduction of gray correlation entropy

The definition of gray entropy was firstly introduced.

Assume $Z = (z_1,z_2,\ldots z_s)$, $\forall i$, $z_s \geqslant 0$, and $\sum z_s = 1$, then the following function

$$H(Z) \triangleq -\sum z_s \ln z_s \tag{7}$$

is defined as the gray entropy of sequence Z, and z_s is attribute information.

The gray entropy of sequence Z has the same structure as the Shannon entropy function. However, there are two differences between them. One of the differences is that the Shannon entropy is a kind of probability entropy and gray entropy is non-probability entropy. The second difference is that gray entropy is gray, while the Shannon entropy is deterministic. The grayness of gray entropy is determined by the grayness of the gray sequence. The attribute information z_s in the gray sequence is completely different from the probability information p_s in the Shannon entropy information space. For a given information space, p_s is a definite value, and z_s can only be regarded as a realistic whitening point of the gray sequence [24,30].

Gray correlation entropy is a kind of gray entropy, and gray correlation entropy of X_i is introduced as follows:

$$H(R_i) \triangleq -\sum_{h=1}^{n} P_h \ln P_h \tag{8}$$

The entropy law shows that when the gray correlation entropy of the sequence is maximal, it means that the distances between the points are more equal to each reference point, that is, X_i is closer to the geometry of the reference sequence, and X_i is the strongest correlation sequence.

3.3. Entropy correlation degree

The entropy correlation degree of sequence X_i is

$$E(x_i) \underline{\underline{\Delta}} H(R_i)/H_m \tag{9}$$

wherein H_m is maximum value of gray entropy and $H_m(x) = \ln n$ represents the maximum entropy of discrepancy information column consisting of n attribute elements.

According to the entropy correlation criterion, the greater the entropy correlation degree of the comparison sequence is, the stronger the correlation between the comparison sequence and the reference sequence will be. The greatest entropy correlation degree indicates that the change of the comparison sequence is closest to the change of the reference sequence. Therefore, using the above model, the dynamic stability of the bio-asphalt mixture was taken as the reference sequence while the indicators of bio-asphalt binder were taken as the comparison sequence, thus the

degree of correlation between the bio-asphalt binder and the dynamic stability of the mixture was determined.

4. Results and discussion

4.1. Test results of binder and mixture of bio-asphalt

The conventional performance test and the Superpave performance test of different test samples before and after the rolling thin film oven (RTFO) aging were carried out. The test samples conclude the 50 penetration grade virgin asphalt (that is 50#), asphalt S100 and bio-asphalt S105, S110, S105 and S120 binders. In addition, the rutting tests of the different mixtures were conducted.

Fig. 3 shows the penetration of different asphalt binders before and after RTFO. And it may have a closer relationship to the deformation resistance.

As shown in Fig. 4, before RTFO, compared with S100, the penetration of bio-asphalt at 25 °C increased by 2.2%, 10.8%, 15.6% and 21%, respectively, with the increase in bio-oil content before RTFO. This showed that with the incorporation of bio-oil, asphalt became soft, its high temperature performance had a certain degree of reduction. After RTFO, when the bio-oil content was 5%, the penetration of bio-asphalt reduced compared with S100, but the reduction was minimal, when the bio-oil content was 10%, the penetration increased, and gradually decreased from S110, and the difference of the penetration before and after RTFO increased with the increase in bio-oil. This indicated that with the increase in bio-oil content, the aging degree of bio-asphalt gradually increased, but the aging was relatively low when the bio-oil content was 10%.

The softening point of different asphalt binders before and after RTFO is shown in Fig. 5. Before RTFO, compared with S100, the softening point decreased by 2.7%, 2.9%, 3.1% and 5.3%, respectively, with the increase in bio-oil content. After RTFO, the softening point of bio-asphalt increased with the increase in bio-oil content. The softening point of bio-asphalt showed the opposite of the law of change before and after short-term aging, this is due to the presence of bio-asphalt after heating to a certain degree of aging. The same trend was found in previous studies as regards the effect of bio-oil content on asphalt aging [31,32].

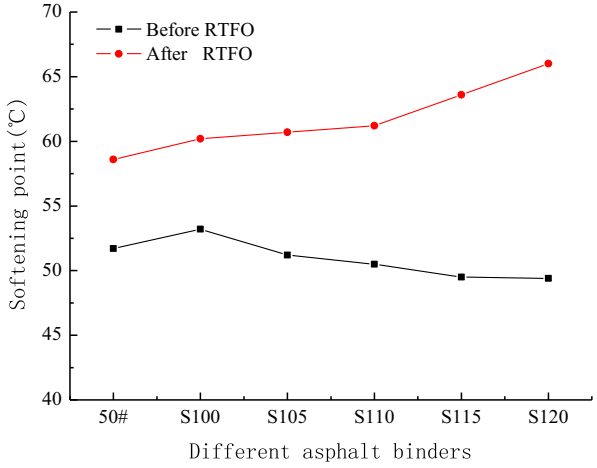

Fig. 5. Softening point of different asphalt binders before and after RTFO.

The mass loss of different asphalt binders after RTFO is shown in Fig. 6. As can be seen from Fig. 6: With the increase in bio-oil content, the mass loss of bio-asphalt increases, indicating that the addition of bio-oil causes the asphalt to be aged. The mass loss of S100, S105 and S110 was −0.286%, −0.357% and −0.57% respectively, which satisfies the requirements of Technical Specification for Construction of Highway Asphalt Pavements (JTG F40-2004) [18], while the mass loss of S115 and S120 could not satisfy the specification.

Fig. 7 shows the viscosity at 135 °C of different asphalt binders. When the SBS was added to the virgin asphalt, the dynamic viscosity of S100 at 135 °C increased. Compared with S100, the dynamic viscosity at 135 °C gradually decreased with the increase in the bio-oil content. It showed a good law of change.

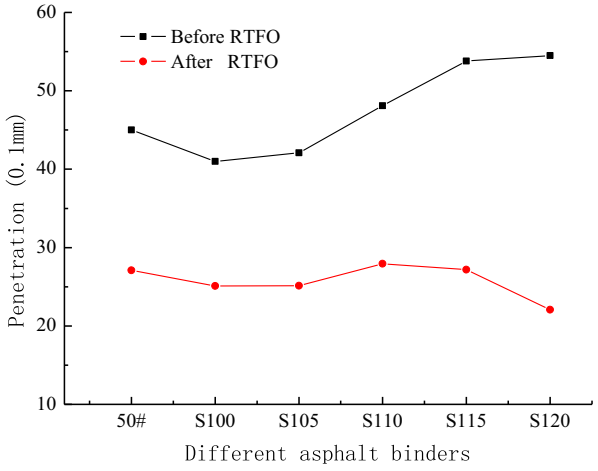

Fig. 4. Penetration of different asphalt binders before and after RTFO.

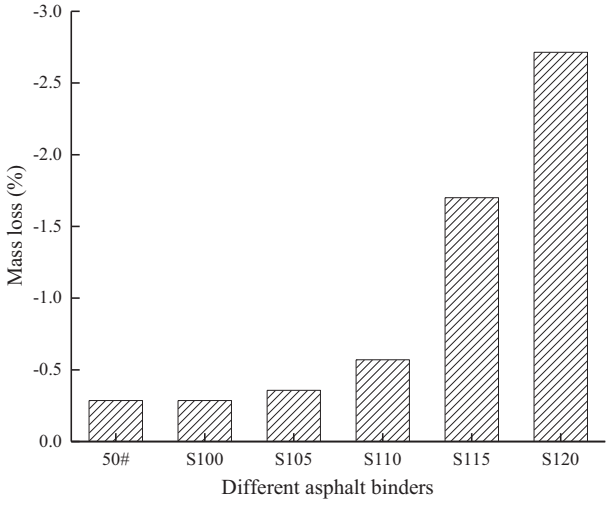

Fig. 6. Mass loss of different asphalt binders after RTFO.

Fig. 8 and Fig. 9 show $G^*/\sin\delta$ and $G^*/(\sin\delta)^9$ before and after RTFO at 64 °C. As shown in Fig. 8 and Fig. 9, $G^*/\sin\delta$ and $G^*/(\sin\delta)^9$ had the same law of change, and $G^*/(\sin\delta)^9$ had a greater temperature sensitivity [20]. $G^*/(\sin\delta)^9$ was selected to analyze the change with the addition of bio-oil. Before the short-term aging, $G^*/(\sin\delta)^9$ decreased with the increase in bio-oil content, however, when the bio-oil content was 20%, $G^*/(\sin\delta)^9$ increased by 7.8% compared with that of the 15% content of bio-oil, which was due to the variation of bio-oil and the addition of bio-oil. $G^*/(\sin\delta)^9$ was the largest after short-term aging when the bio-oil content was 10%. It was shown that the anti-rutting ability of bio-asphalt S110 was the largest after aging.

As can be seen from Fig. 10, with the increase in bio-oil content, bio-asphalt's non-recoverable creep compliance showed a downward trend, this showed that after short-term aging, the incorporation of bio-oil could increase the anti-rutting deformation ability of bio-asphalt. The unrecoverable creep compliance of S115 was larger than that of S110 and S120, which was due to the variation of its performance after short-term aging when the bio-oil content was 15%. Meanwhile, at the stress level of 3.2 kPa, the non-recoverable creep compliance of different asphalt was larger than that of 0.1 kPa stress level, which indicated that the anti-rutting ability of the asphalt is affected by the stress generated by the vehicle load on the road.

Fig. 11 shows the dynamic stability of different asphalt binders. As can be seen from Fig. 11, when the bio-oil was added to S100 asphalt binder, the dynamic stability of bio-asphalt mixtures was lower than the base asphalt mixture, while the dynamic stability of bio-asphalt mixtures decreased with the increase in bio-oil content.

From the analysis of the test results of conventional performance test and the Superpave performance test of different test samples before and after the rolling thin film oven, different parameters such as penetration, softening point, $G^*/\sin\delta$ at 64 °C before and after RTFO, $G^*/(\sin\delta)^9$ at 64 °C before and after RTFO, $J_{nr3.2}$ and $J_{nr0.1}$ at 64 °C showed different changes in the law with the changes of bio-oil content. The fact of how to further characterize

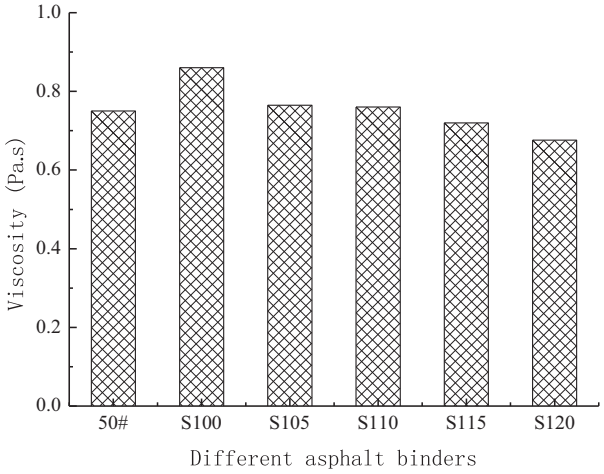

Fig. 7. Viscosity at 135 °C of different asphalt binders.

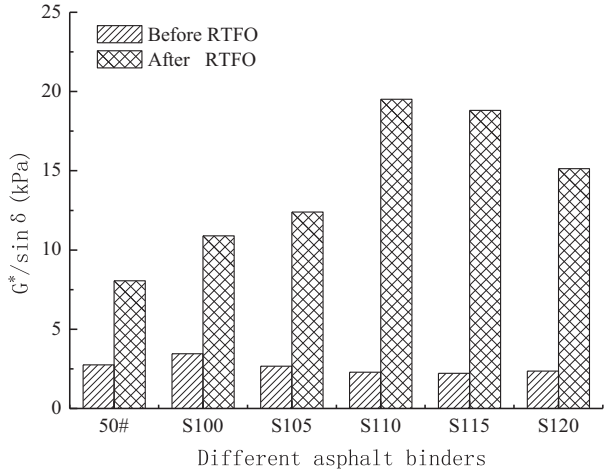

Fig. 8. $G^*/\sin\delta$ of different asphalt binders before and after RTFO.

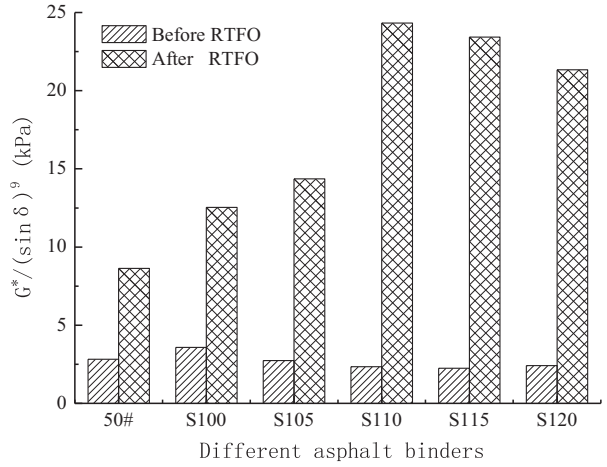

Fig. 9. $G^*/(\sin\delta)^9$ of different asphalt binders before and after RTFO.

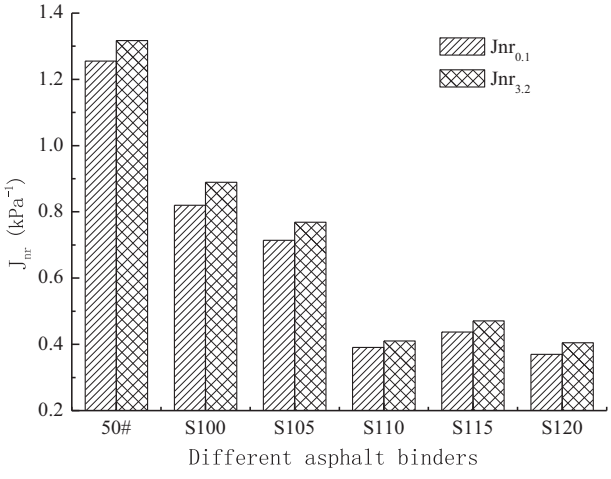

Fig. 10. Unrecoverable creep compliance of different asphalt binders at 64 °C.

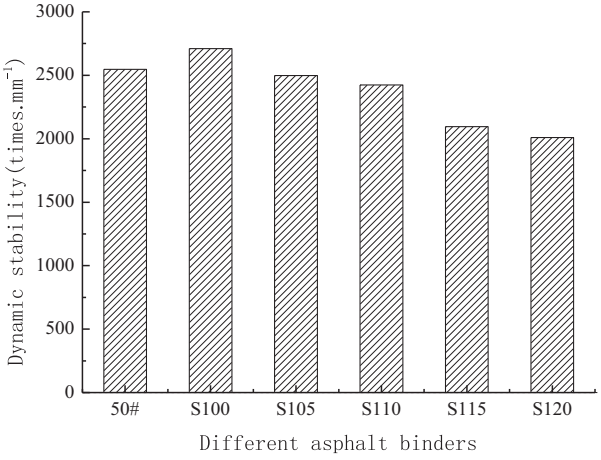

Fig. 11. Dynamic stability of different asphalt binders.

the high temperature performance of bio-asphalt needs further analysis.

4.2. Gray relational analysis between binder and mixture of bio-asphalt

In order to further analyze high temperature performance of bio-asphalt and to better analyze the relation between the binder and the mixture, the results of different asphalt binders and asphalt mixtures were numbered from 0 to 11 and listed in Table 5.

The dynamic stability X_0 of bio-asphalt mixture was taken as the reference sequence while the indexes of bio-asphalt binder shown in Table 5 were taken as the comparison sequence, the indicators listed in Table 5 from top to bottom were defined as $X_1$to X_{11}. Then the data normalization was taken, the results are presented in Table 6.

The absolute difference between the two sequences was calculated according to the sequence generated by the equalization method in Table 6, and the gray relational coefficients were calculated, as shown in Table 7.

Fig. 12 shows the entropy correlation degree between asphalt binder indicators and dynamic stability of bio-asphalt mixtures. They were successively shown as follows: $E(x_1) = 0.9925$, $E(x_2) = 0.9981$, $E(x_3) = 0.9983$, $E(x_4) = 0.9953$, $E(x_5) = 0.9988$, $E(x_6) = 0.9962$, $E(x_7) = 0.9928$, $E(x_8) = 0.9959$, $E(x_9) = 0.9949$, $E(x_{10}) = 0.9741$, $E(x_{11}) = 0.9716$. As can be seen, $E(x_5) > E(x_3) > E(x_2) > E(x_6) > E(x_8) > E(x_4) > E(x_9) > E(x_7) > E(x_1) > E(x_{10}) > E(x_{11})$, that is, dynamic viscosity at 135 °C > Penetration at 25 °C after RTFO > softening point before RTFO > $G^*/\sin\delta$ at 64 °C before RTFO > $G^*/(\sin\delta)^9$ at 64 °C before RTFO > softening point after RTFO > $G^*/(\sin\delta)^9$ at 64 °C after RTFO > $G^*/\sin\delta$ at 64 °C after RTFO > Penetration at 25 °C before RTFO > $J_{nr3.2}$ at 64 °C > $J_{nr0.1}$ at 64 °C. According to the entropy correlation criterion, the greater the entropy correlation degree of the indicators of bio-asphalt binder's high temperature is, the stronger the correlation between the indicators of bio-asphalt binder's high temperature performance and the dynamic stability reflecting the high temperature performance of asphalt mixtures will be. Because the dynamic stability could well reflect the high temperature performance of the asphalt mixture, the greater the correlation of indicators with the dynamic stability is, the better the indicators could characterize the high temperature performance of the binder. Therefore, the dynamic viscosity at 135 °C had the highest correlation with the dynamic stability, penetration after RTFO and the softening point before RTFO were second, and the correlation of $J_{nr3.2}$ and $J_{nr0.1}$ at 64 °C were the least correlated with dynamic stability Table 8.

In order to more intuitively explain the application of gray relational entropy analysis method, according to Table 6, the normalized data of reference sequence and six representative sequences, X_0 (Dynamic stability), X_5 (Dynamic viscosity at 135 °C), X_3 (Penetration at 25 °C after RTFO), X_2 (Softening point before RTFO), X_1 (Penetration at 25 °C before RTFO), X_{10} ($J_{nr3.2}$ at 64 °C), X_{11} ($J_{nr0.1}$ at 64 °C), were selected to be compared in one figure, as shown in Fig. 13. As can be seen from the figure, the closest change (the geometric shape of the curve) to X_0 was X_5, followed by X_3 and X_2, while the change (the geometric shape of the curve) of X_{11} was the most different from X_0. This also showed that entropy correlation degree can accurately characterize the relationship between different comparison sequences and the reference sequence.

Table 5
Results of different asphalt binders and asphalt mixtures.

Parameters	NO.	50#	S100	S105	S110	S115	S120
Dynamic stability/timesṁm^{-1}	0	2546.55	2710.62	2497.32	2423.08	2095.78	2010.21
Penetration at 25 °C before RTFO/0.1 mm	1	53.00	50.00	51.10	55.40	57.80	60.50
Softening point before RTFO/°C	2	49.50	51.00	49.60	49.50	49.40	48.30
Penetration at 25 °C after RTFO/0.1 mm	3	36.25	34.25	33.88	36.07	29.21	24.49
Softening point after RTFO/°C	4	55.60	57.20	57.90	58.20	63.60	66.00
Dynamic viscosity at 135 °C/(Paṡs)	5	0.75	0.86	0.765	0.76	0.72	0.676
$G^*/\sin\delta$ at 64 °C before RTFO/kPa	6	2.754	3.447	2.666	2.290	2.219	2.365
$G^*/\sin\delta$ at 64 °C after RTFO/kPa	7	8.062	10.890	12.400	19.510	18.810	15.130
$G^*/(\sin\delta)^9$ at 64 °C before RTFO/kPa	8	2.817	3.583	2.734	2.340	2.246	2.421
$G^*/(\sin\delta)^9$ at 64 °C after RTFO/kPa	9	8.636	12.537	14.354	24.327	23.434	21.330
$J_{nr3.2}$ at 64 °C /kPa^{-1}	10	1.317	0.889	0.769	0.410	0.471	0.405
$J_{nr0.1}$ at 64 °C /kPa^{-1}	11	1.255	0.820	0.714	0.391	0.437	0.370

Table 6
The sequence generated by the normalization.

Parameters	$X_{NO.}$	50#	S100	S105	S110	S115	S120
Dynamic stability/timesmm^{-1}	X_0	1.07	1.14	1.05	1.02	0.88	0.84
Penetration at 25 °C before RTFO/0.1 mm	X_1	0.97	0.92	0.94	1.01	1.06	1.11
Softening point before RTFO/°C	X_2	1.00	1.03	1.00	1.00	1.00	0.97
Penetration at 25 °C after RTFO/0.1 mm	X_3	1.12	1.06	1.05	1.11	0.90	0.76
Softening point after RTFO/°C	X_4	0.93	0.96	0.97	0.97	1.06	1.10
Dynamic viscosity at 135 °C/(Paṡs)	X_5	0.99	1.14	1.01	1.01	0.95	0.90
$G^*/\sin\delta$ at 64 °C before RTFO/kPa	X_6	1.05	1.31	1.02	0.87	0.85	0.90
$G^*/\sin\delta$ at 64 °C after RTFO/kPa	X_7	0.57	0.77	0.88	1.38	1.33	1.07
$G^*/(\sin\delta)^9$ at 64 °C before RTFO/kPa	X_8	1.05	1.33	1.02	0.87	0.83	0.90
$G^*/(\sin\delta)^9$ at 64 °C after RTFO/kPa	X_9	0.50	0.72	0.82	1.40	1.34	1.22
$J_{nr3.2}$ at 64 °C /kPa^{-1}	X_{10}	1.85	1.25	1.08	0.58	0.66	0.57
$J_{nr0.1}$ at 64 °C /kPa^{-1}	X_{11}	1.89	1.23	1.07	0.59	0.66	0.56

Table 7
Gray relational coefficients between asphalt indexes and dynamic stability.

Parameters	50#	S100	S105	S110	S115	S120
r_1	0.8047	0.6473	0.7830	0.9912	0.6978	0.6092
r_2	0.8531	0.7896	0.8954	0.9564	0.7787	0.7589
r_3	0.8905	0.8366	0.9956	0.8091	0.9487	0.8242
r_4	0.7467	0.6934	0.8370	0.9038	0.6902	0.6117
r_5	0.8429	1.0000	0.9196	0.9733	0.8490	0.8901
r_6	0.9539	0.7006	0.9262	0.7389	0.9226	0.8781
r_7	0.4508	0.5268	0.7049	0.5306	0.4764	0.6446
r_8	0.9482	0.6797	0.9264	0.7348	0.9005	0.8810
r_9	0.4164	0.4941	0.6448	0.5207	0.4692	0.5196
r_{10}	0.3431	0.7846	0.9243	0.4821	0.6537	0.5997
r_{11}	0.3335	0.8114	0.9419	0.4883	0.6480	0.5877

The density value of distribution was calculated based on the gray relational coefficient, and the gray relational entropy was calculated as shown in Table 8.

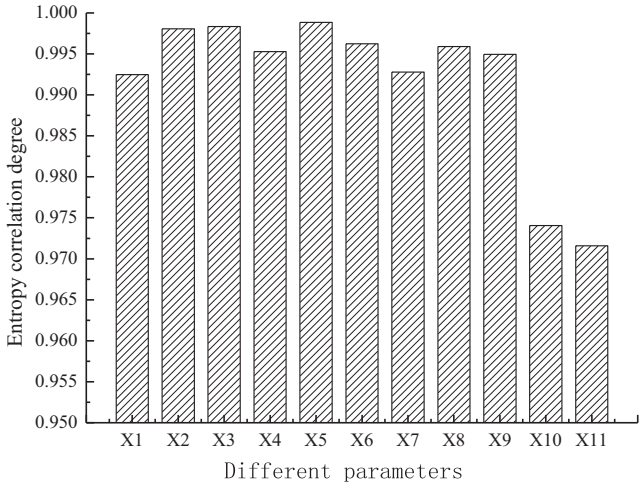

Fig. 12. Entropy correlation degree between asphalt indicators and dynamic stability of bio-asphalt.

The analyses above showed that: (1) The irreversible creep compliance J_{nr} had a good correlation with the rutting performance of polymer modified asphalt [33], but the content of SBS modifier in this study was lower than that of conventional SBS modified asphalt (3–6%) [34,35], which may be the reason for the weak correlation between the creep compliance and dynamic stability. (2) In the determination of rutting factor, the frequency of load had some difference with the actual conditions on the road, and its determination was based on linear viscoelasticity. The viscosity of bio-asphalt was large, therefore, there were some shortcomings using the rutting factor and $G^*/(\sin\delta)^9$ to evaluate the high temperature performance of the bio-asphalt in this study, and the relevance ranking was relatively centered. (3) Softening point characterizes the temperature at the same viscosity, and it has a weak correlation with the high temperature performance of asphalt pavement, although the softening point before RTFO was relatively advanced, it was not sufficient to regard it as a key indicator. (4) The entropy correlation degree ranking of penetration before and after RTFO were 9 and 2, respectively; the rank of softening point before and after RTFO was 3 and 6, respectively; the rankings of $G^*/\sin\delta$ before and after RTFO were 4 and 8, respectively; the rankings of $G^*/(\sin\delta)^9$ ranking before and after RTFO were 5 and 7, respectively. The order of the above indexes changed greatly, it was shown that the aging of RTFO had a great influence on the performance of bio-asphalt, and the influence of aging should be taken into account in the performance analysis. (5) The viscosity of asphalt could reflect the ability of asphalt pavement to resist rutting at high temperatures, the larger the value, the smaller the shear deformation under loads. The dynamic viscosity of 135 °C not only reflected the high temperature performance of asphalt but also reflected the situation of bio-asphalt after a certain degree of aging, and it had the best correlation

Table 8
Gray relational entropy between asphalt indexes and dynamic stability.

Parameters	$H(R_1)$	$H(R_2)$	$H(R_3)$	$H(R_4)$	$H(R_5)$	$H(R_6)$	$H(R_7)$	$H(R_8)$	$H(R_9)$	$H(R_{10})$	$H(R_{11})$
Gray relational entropy	1.7783	1.7883	1.7888	1.7833	1.7897	1.7850	1.7788	1.7844	1.7827	1.7453	1.7408

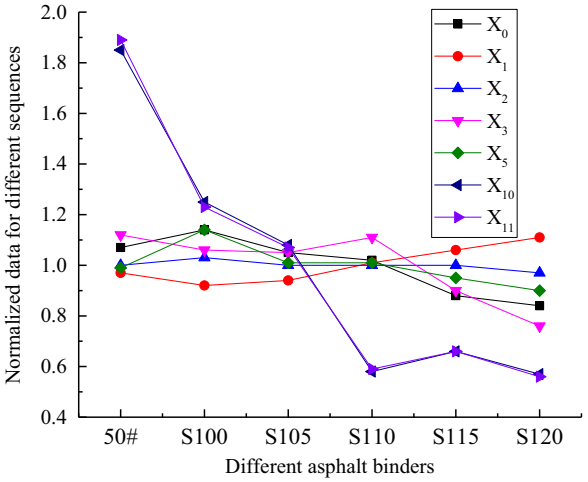

Fig. 13. The changes of the comparison sequences and reference sequence based on normalized data.

with the dynamic stability of the mixture in the gray correlation entropy analysis. Therefore, it could be used as the key index of high-temperature performance evaluation of bio-asphalt.

5. Conclusion

In this study, to analyze the gray relational entropy of high temperature performance of bio-asphalt binder and its mixture, the performance indexes of the asphalt binder and the dynamic stability of the mixture were tested, and the correlation between the indexes of the asphalt binder and the dynamic stability of the mixture was studied through the gray correlation entropy method. From these test results, the following conclusions were drawn:

(1) With the incorporation of bio-oil, the penetration of bio-asphalt increased and the softening point decreased before RTFO, and the penetration decreased and the softening point increased after RTFO. The bio-asphalt became soft and its high temperature performance had a certain degree of reduction before RTFO. While it became hard after RTFO, which was due to the aging of the addition of some bio-oil.

(2) The dynamic viscosity at 135 °C gradually decreased with the increase in the bio-oil content. It showed a good law of change. $G^*/(\sin\delta)^9$ was the largest after short-term aging when the bio-oil content was 10%. The anti-rutting ability of bio-asphalt S110 was the largest after aging. With the increase in bio-oil content, bio-asphalt's non-recoverable creep compliance showed a downward trend.

(3) The dynamic stability of bio-asphalt mixtures decreased with an increase in bio-oil content. The binder test parameters showed different changes in the law with the changes of bio-oil content.

(4) The ranking of the entropy correlation degree between asphalt indicators and dynamic stability of bio-asphalt is different. The RTFO aging had a great influence on the entropy correlation between the same performance indexes of the bio-asphalt determined and the dynamic stability of the mixture.

(5) The creep compliance of the bio-asphalt with a low content (1%) of SBS modifier was weakly correlated with the dynamic stability of the mixture. The dynamic viscosity of bio-asphalt and the dynamic stability of the mixture had the highest gray entropy correlation, which could be used as the key indicators of the high-temperature performance evaluation of bio-asphalt.

Acknowledgements

This research is sponsored by the Basic Scientific Research Funds of the National Natural Science Foundation of China (NSFC) (No.51578075), the Fundamental and Applied Research Project of the Chinese National Transportation Department (2014319812180), and the Special Fund for Basic Scientific Research of Central Colleges, Chang'an University (CHD310821153503). The authors also gratefully acknowledge the financial support from China Scholarship Council (No. 201706560009).

References

[1] B. Colberta, M.R. Mohd, Hasan, Z.P. You, A hybrid strategy in selecting diverse combinations of innovative sustainable materials for asphalt pavements, J. Traffic Transport. Eng. (English Edition) 3 (2) (2016) 89–103.
[2] H.N. Wang, J.F. Gao, Z.P. You, et al., Advances in bio-binder application on road pavement, J. Wu Han Univ. Technol. 36 (7) (2014) 57–60 (in Chinese).
[3] M.R. Mohd, Hasan, Z.P. You, Ethanol Based Foamed Asphalt as Potential Alternative for Low Emission Asphalt Technology, J. Traffic Transport. Eng. (English Edition) 3 (2) (2016) 116–126.
[4] Yang, X.,Mills-Beale J., You Z. P.. Chemical Characterization and Oxidative Aging of Bio-asphalt and Its Compatibility with Petroleum Asphalt. Journal of Cleaner Production. 2017,142, Part 4: 1837-1847.
[5] E.H. Fini, E.W. Kalberer, A. Shahbazi, et al., Chemical characterization of bio-binder from swine manure: sustainable modifier for asphalt binder, J. Mater. Civ. Eng. 23 (11) (2011) 1506–1513.
[6] E.H. Fini, I.L. Al-Qadi, Z.P. You, et al., Partial replacement of asphalt binder with bio-binder: characterisation and modification, Int. J. Pavement Eng. 13 (6) (2012) 515–522.
[7] M.B. Julian, Z.P. You, Aging influence on rheology properties of petroleum-based asphalt modified with bio-binder, J. Mater. Civ. Eng. 26 (2) (2014) 358–366.
[8] Onochie, A., Fini, E. H., Yang X.,et al.. Rheological Characterization of Nano-particle based Bio-modified Binder. TRB 2013 Annual Meeting CD-ROM.
[9] X. Yang, Z.P. You, Q. Dai, et al., Mechanical performance of asphalt mixtures modified by bio-oils derived from waste wood resources, Constr. Build. Mater. 51 (2014) 424–431.
[10] X. Yang, Z.P. You, Q. Dai, Performance evaluation of asphalt binder modified by bio-oil generated from waste wood resources, Int. J. Pavement Res. Technol. 6 (4) (2013) 431–439.

[11] Raouf, M. A., Williams, R. C. Determination of Pre-Treatment Procedure Required for Developing Bio-Binders from Bio-Oils. Proceedings of the 2009 Mid-Continent Transportation Research Symposium. Iowa: Ames, Iowa State University.
[12] Yang, S.H., Suciptan, T., Chang, Y. H.. Investigation of Rheological Behavior of Japanese Cedar Based Bio-Binder As Partial Replacement For Bituminous Binder. TRB 2013 Annual Meeting CD-ROM.
[13] H.N. Wang, J.F. Gao, X. Zhao, et al., Rheological properties on bio-binder based on DSR and RV, J. Hu Nan Univ. (Nat. Sci.) 42 (6) (2015) 26–33 (in Chinese).
[14] J.F. Gao, H.N. Wang, Z.P. You, et al., Research on properties of bio-asphalt binders based on time and frequency sweep test, Constr. Build. Mater. 160 (2018) 786–793.
[15] M. He, D.W. Cao, H.Y. Zhang, et al., Study on regular performance of modified bio-asphalt, J. Highway Transport. Res. Dev. 32 (2) (2015) 8–12 (in Chinese).
[16] D. Rodrigo, U.B. Hussain, The relationship between nonlinearity of asphalt binders and asphalt mixture permanent deformation, Road Mater. Pavement Des. 3 (2010) 653–680.
[17] K. Sungun, P. Jiyong, W.K. Kwang, Correlation analyses for implementation of binder properties for rut potential estimation of asphalt mixtures, J. Test. Eval. 39 (2011) 858–867.
[18] Ministry of Transport of the People's Republic of China, Technical Specification for Construction of Highway Asphalt Pavements (JTG F40-2004). China Communications Press, Beijing, 2004 (in Chinese).
[19] Ministry of Transport of the People's Republic of China, Standard Test Methods of Bitumen and Bituminous Mixtures for Highway Engineering (JTG E20-2011). China Communications Press, Beijing, 2011 (in Chinese).
[20] A. Shenoy, Unifying asphalt rheological data using the material's volumetric-flow rate, J. Mater. Civ. Eng. 13 (2001) 260–273.
[21] AASHTO TP 70-10, Stand Method of Test for Multiple Stress Creep Recovery (MSCR) Test of Asphalt Binder using a Dynamic Shear Rheometer (DSR).
[22] X. Yang, Z.P. You, High temperature performance evaluation of bio-oil modified asphalt binders using the DSR and MSCR tests, Constr. Build. Mater. 76 (2015) 380–387.
[23] J.L. Deng, Introduction to Grey Mathematical Resource Science, Huazhong University of Science and Technology Press, Wuhan, 2010.
[24] Q.S. Zhang, X.J. Guo, J.L. Deng, Gray correlation entropy analysis method, Syst. Eng. Theory Practice 8 (1996) 7–11 (in Chinese).
[25] Z.X. Wang, Y.G. Dang, M.X. Cao, Weighted degree of grey incidence based on optimized entropy, Syst. Eng. Electron. 32 (4) (2010) 774–783 (in Chinese).
[26] Y.J. Tong, B.X. Shen, J.C. Liu, et al., Characterization of hard-grade asphalt using entropy analysis, Pet. Sci. Technol. 35 (2017) 703–709.
[27] S.Y. Zhu, S.F. Chen, X.T. Qin, et al., Key indexes of high viscosity modified asphalt based on grey correlation entropy analysis 867 867, J. Mater. Sci. Eng 32 (6) (2014) (in Chinese).
[28] Y.J. Tong, B.X. Shen, J.C. Liu, et al., Characterization of hard-grade asphalt using entropy analysis, Pet. Sci. Technol. 35 (7) (2017) 703–709.
[29] Z.J. Wang, Q. Wang, T. Ai, et al., Comparative study on effects of binders and curing ages on properties of cement emulsified asphalt mixture using gray correlation entropy analysis, Constr. Build. Mater. 54 (2014) 615–622.
[30] J.W. Godden, J. Bajorath, et al., Differential shannon entropy as a sensitive measure of differences in database variability of molecular descriptors, J. Chem. Inf. Model. 41 (4) (2001) 1060–1066.
[31] R. Zhang, H.N. Wang, J.F. Gao, et al., High temperature performance of SBS modified bio-asphalt, Constr. Build. Mater. 144 (2017) 99–105.
[32] X. Yang, Z.P. You, J. Mills-Beale, Asphalt binders blended with high percentage of bio-binders: aging mechanism using FTIR and rheology, J. Mater. Civ. Eng. 27 (4) (2014) 1–11.
[33] D'angelo J. The Relationship of the MSCR Test to Rutting. Road Materials and Pavement Design, 2009, 10(S1), 61-80.
[34] A.K. Swamy, U.D. Rongali, P.K. Jain, Effect of HDPEH polymer on viscoelastic properties of SBS modified asphalt, Construct. Build. Mater. 136 (2017) 230–236.
[35] J.Q. Zhu, B. Birgisson, N. Kringos, Polymer modification of bitumen: advances and challenges, Eur. Polym. J. 54 (2014) 18–38.